第 27 卷第 1 期 无 机 化 学 学 报 Vol.27 No.1
2011 年 1 月 CHINESE JOURNAL OF INORGANIC CHEMISTRY 167-173

$(TCNQ)_2^{2-}$基氢键分子磁体表现出非常强的反铁磁偶合作用

袁国军[1] 赵顺平[1] 任小明*,[1,2] 孟庆金[2] 房晨婕*,[3]
([1]南京工业大学应用化学系,南京 210009)
([2]南京大学配位化学研究所,配位化学国家重点实验室,南京 210093)
([3]首都医科大学化学生物学与药学院,北京 100069)

摘要: 合成并表征了一种新的离子对化合物 [4-NH_2-Py][TCNQ](其中 4-NH_2-Py^+是 4-氨基吡啶阳离子,$TCNQ^-$为 7,7,8,8-四氰基对苯二醌二甲烷自由基阴离子)。在该离子对化合物晶体中,2 个 $TCNQ^-$离子形成了面对面堆积的二聚体;阴离子中的氰基分别和阳离子上的氨基、吡啶质子化氮原子之间存在非常强的分子间氢键。通过氢键作用,相邻的 $TCNQ^-$二聚体被阳离子连成三维氢键网络。变温磁化率测量表明,在 2~400 K 温度范围内,该离子对化合物表现为抗磁性。在密度泛函理论框架下,用对称性破损方法计算了化合物晶体中 π 二聚体内以及通过氢键连接的相邻的 $TCNQ^-$离子之间的磁交换常数,发现 π 二聚体内存在非常强的反铁磁交换作用, 与之相比, 通过氢键连接的 $TCNQ^-$离子之间的磁交换作用可以忽略。π 二聚体内强反铁磁交换作用($J/k_B \approx 1\,805$ K)导致了该化合物基本表现为抗磁性。

关键词: 离子对; 晶体结构; 磁性; DFT 计算; 对称性破损
中图分类号: O646.8; O641.4 **文献标识码**: A **文章编号**: 1001-4861(2011)01-0167-07

Very Strong Antiferromagnetic Coupling Interaction in $(TCNQ)_2^{2-}$ Spin Dimers H-bonding Molecular Magnetic Compound

YUAN Guo-Jun[1] ZHAO Shun-Ping[1] REN Xiao-Ming*,[1,2] MENG Qing-Jin[2] FANG Chen-Jie*,[3]
([1]*Department of Applied Chemistry, College of Science, Nanjing University of Technology, Nanjing* 210009, *China*)
([2]*Coordination Chemistry Institute & State Key Lab, Nanjing University, Nanjing* 210093, *China*)
([3]*College of Chemical Biology and Pharmaceutical Sciences, Capital Medical University, Beijing* 100069, *China*)

Abstract: An ion-pair type of hydrogen bonding molecular magnetic compound was prepared by means of combining the paramagnetic $TCNQ^-$ (TCNQ=7,7,8,8-tetracyanoquinodimethane) and nonmagnetic 4-aminopyridinium. The single crystal structure of the title compound shows two $TCNQ^-$ anions form an isolated -type $(TCNQ)_2^{2-}$ dimer, and the adjacent $(TCNQ)_2^{2-}$ dimers are connected by 4-aminopyridinium via strong hydrogen-bonding. The variable temperature magnetic susceptibility measurement in the temperature range of 2~400 K indicates diamagnetism characteristics of the compound. The magnetic coupling constants between the neighboring $TCNQ^-$ anions were evaluated by the broken-symmetry approach in the density functional theory (DFT) framework. The results reveal that the strong antiferromagnetic coupling interaction ($J/k_B \approx 1\,805$ K) within the π-type $(TCNQ)_2^{2-}$ dimer gives rise to the diamagnetism behavior for this ion-pair compound. CCDC: 779452.

Key words: ion pairs; crystal structure; magnetic property; DFT calculation; broken-symmetry

收稿日期:2010-07-12。收修改稿日期:2010-09-10。
国家自然科学基金(No.20871068)资助项目。
*通讯联系人。E-mail:xmren@njut.edu.cn

0 Introduction

Molecule-based magnets have been attracted a great deal of academic interests, and lots have been achieved over the past three decades, for example, the critical temperature, T_C, higher than room temperature magnets [1-3], hard magnet with giant coercivity (a coercive field of 52 kOe) [4], spin transition with multiple stability material [5], magneto-opto-Electronic bistability material [6], conducting ferromagnet [7], giant negative magnetoresistance material [8] as well as single-molecule [9-10] or single-chain [11] magnets with macroscopic quantum tunneling magnetization have been discovered. In our previous studies, the supramolecular crystal engineering method was utilized to create a series of one-dimensional quantum magnetic chain systems based on the paramagnetic molecular architecture, $[Ni(mnt)_2]^-$ (where mnt^{2-} represents maleonitriledithiolate), and the systems exhibit novel spin-Peierls-type magnetic transition [12]. Another finding is that -CN groups of mnt^{2-} ligands are potential hydrogen bond acceptors. The H-bonding interactions between $[Ni(mnt)_2]^-$ anions and counterions could have strong influence on the arrangement of $[Ni(mnt)_2]^-$ anions and the magnetic property of the corresponding molecular magnet. When a strong hydrogen bond donor-type counterion is introduced into $[Ni(mnt)_2]^-$ system, a spin transition system with bistability [13] and long range ferromagnetic ordering system[14] are obtained, respectively, since the hydrogen bond interactions between $[Ni(mnt)_2]^-$ anions and counterions enhance the cooperative magnetic interactions between the paramagnetic $[Ni(mnt)_2]^-$ anions.

As shown in Scheme 1, the organic radical anion, $TCNQ^-$ (TCNQ=7,7,8,8-tetracyanoquinodimethane), possesses similar molecular and electronic structures with the $[Ni(mnt)_2]^-$ anion, for example, both anions are planar with extended electronic structure, moreover, both anions have four -CN groups which can be employed as potential hydrogen bond acceptors. It is expected to create $TCNQ^-$-based H-bonding molecular magnet with novel magnetic property when a potential hydrogen bond donor-type cation, 4-aminopyridinium (4-NH_2-Py^+), is introduced into $TCNQ^-$ spin system.

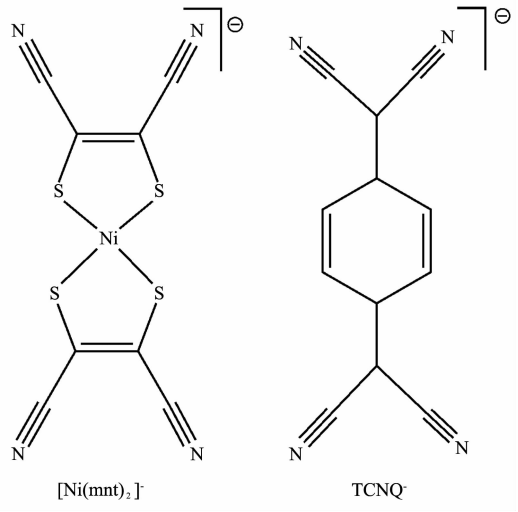

Scheme 1 Molecular structures of $[Ni(mnt)_2]^-$ and $TCNQ^-$ anions

Herein we report a $(TCNQ)_2^{2-}$-based H-bonding molecular magnetic compound, which shows very strong antiferromagnetic coupling interaction within a $(TCNQ)_2^{2-}$ spin dimer.

1 Experimental

1.1 Chemicals and materials

All chemicals and solvents were reagent grade and used without further purification. Li(TCNQ) and 4-aminopyridinium chloride ([4-NH_2-Py]Cl) were synthesized following the published procedures[14-15].

1.2 Physical measurements

Elemental analyses for C, H and N were performed with an Elementar Vario EL III analytic instrument. IR spectra were recorded on a Bruker Vector 22 Fourier Transform Infrared Spectrometer (170SX) (KBr disc). Powder X-ray diffraction (PXRD) data for **1** were collected on a RigaKu/max-2550 diffractometer with Cu $K\alpha$ radiation with λ=0.154 18 nm at room temperature. The acceleration voltage was 40 kV with a 40 mA current flux. Scatter and diffraction slits of 0.5 mm and collection slits of 0.3 mm were used and data were collected in the 2θ range from 5° to 50°, with a scanning rate of 4°·min and a sample interval of 0.02°. Magnetic susceptibility

data on polycrystalline sample were collected over the temperature range of 2 ~400 K using a Quantum Design MPMS-XL superconducting quantum interference device (SQUID) magnetometer and the diamagnetism correction was performed by Pascals constants[16].

1.3 Preparation of[4-NH_2-Py][TCNQ] (1)

[4-NH_2-Py][TCNQ] (**1**). [4-NH_2-Py]Cl (131 mg, 1 mmol) and LiTCNQ (211 mg, 1 mmol) were mixed under stirring in EtOH (25 mL) at room temperature, and the immediately formed purple microcrystal product was filtered off, washed with EtOH and then dried in vacuum at room temperature to give 233 mg of **1**, yield was 78%. Elemental analysis: found: C, 67.8, H, 3.75, N, 27.9% and calculated for $C_{17}H_{11}N_6$: C, 68.2; H 3.70; N, 28.1%. IR spectrum (cm^{-1}): the bands at 2 210 (vs) and 2 223 (vs) are attributed to v(CN) of $(TCNQ)^-$.

The single crystals suitable for X-ray analysis were obtained via layering, namely, the more dense EtOH solution of Li (TCNQ) was added to the bottom of test tube and the less dense EtOH solution of [4-NH_2-Py]Cl was layered on the top of the EtOH solution of Li (TCNQ); the single crystals were gained after 10 days.

1.4 X-ray crystal structure analysis

The single crystal X-ray diffraction data for **1** were collected at 296 K with graphite-monochromatized Mo $K\alpha$ (λ=0.071 073 nm) on an Enraf-Nonius CAD4 type of four-circle diffractometer. Structure was solved by the direct method and refined by the full-matrix least squares procedure on F^2 using SHELX-97 program [17]. All non-hydrogen atoms were refined anisotropically, and the hydrogen atoms were introduced at calculated passions, the crystallographic details about data collection and structure refinement are summarized in Table 1.

CCDC: 779452.

Table 1　Crystallographic and structure refinement data of 1

Chemical formula	$C_{17}H_{11}N_6$	Density / ($g\cdot cm^{-3}$)	1.351
Formula weight	299.32	Abs.coeff. / mm^{-1}	0.087
Temperature / K	293(2)	F(000)	620
Wavelength / nm	0.710 73	θ ranges (data collection) / (°)	1.43~25.25
Space group	$P2_1/c$	Index ranges	$-19\leqslant h\leqslant 17$; $0\leqslant k\leqslant 8$; $0\leqslant l\leqslant 16$
a / nm	1.585 5(3)	R_{int}	0.032 1
b / nm	0.728 80(15)	Independent reflections/restraints/parameters	2 652/9/208
c / nm	1.418 6(3)	Refinement method	Least square refinement on F^2
α / (°)	90	Goodness-of-fit on F^2	1.057
β / (°)	116.18(3)	Final R indices [$I>2\delta(I)$]	R_1=0.081 5, wR_2=0.115 1
γ / (°)	90	R indices(all data)	R_1=0.207 9, wR_2=0.145 8
V / nm^3	1.471 0(5)	Residual / ($e\cdot nm^{-3}$)	193/−166
Z	4		

$R_1=\sum(||F_o|-|F_c||)/\sum|F_o|$, $wR_2=\sum w(|F_o|^2-|F_c|^2)^2/\sum w(|F_o|^2)^2]^{1/2}$

1.5 DFT calculation details

All density functional theory (DFT) calculations were carried out utilizing the Gaussan98 program[18]. The single point energy calculations of the triplet and broken-symmetric states for each spin dimer of $(TCNQ)_2^{2-}$ in **1** were performed on the non-modelized molecular geometry from single crystal X-ray analysis, and the SCF convergence criterion is 10^{-8} (in some cases, SCF convergence difficulties could be alleviated by decreasing the convergence criterion of SCF to 10^{-6}). In this study, the several DFT functionals, such as the local spin density approach (svwn) [19-20], the generalized gradient approximations (bpw91[21-22]) and the hybrid functional methods (b3lyp, b3pw91) [23-24] with the 6-31 +g (d,p) basis sets were employed. Judging by the magnetic exchange constant J values, it was found that the DFT functional bpw91 with the 6-31 +g (d,p) basis sets could provide

reasonable results. Therefore, the calculations performed at the ubpw91 level with 6-31+g(d,p) basis sets are used for discussion in this paper.

2 Results and discussion

2.1 Description of crystal structure

Compound **1** crystallizes as a monoclinic system with space group of $P2_1/c$. An asymmetric unit contains one $TCNQ^-$ anion with one 4-NH_2-Py^+ cation (as shown in Fig.1). The mean-molecule-plane of $TCNQ^-$ ion with the eight heavy atoms of the quinodimethane group is tilted with respect to the pyridyl ring of the cation, with the dihedral angle of 28.1 between the two molecular planes. The averaged lengths of chemically similar bonds in the $TCNQ^-$ ion are listed in Table 2, and their values are close to those in the reported $TCNQ^-$ compounds [25-29]. Two types of strong intermolecular H-bonding interactions are observed between the anions and the cations, as depicted in Fig.2, each NH_2- group of the cation, as a H-bonding donor, connects two NC- groups (H-bonding acceptor) from two neighboring TCNQ anions with H-bonding parameters of $d_{N(6)...N(4)}$=0.292 3 nm, ∠N(4)...H(6C)-N(6)=145.1°, $d_{N(6)...N(3\#1)}$=0.3079 nm, ∠N(3#1)...H(6B)-N(6)=161.5°(symmetric code #1: x, $-1+y$, z); and each protonated N-atom of the pyridium forms a bifurcated hydrogen bond with two adjacent TCNQ anions with H-bonding parameters of $d_{N(5)...N(1\#2)}$= 0.305 8 nm, ∠N(1#2)...H(5B)-N(5)=134.1°, $d_{N(5)...N(2\#3)}$= 0.335 4 nm, ∠N(2#3)...H(5B)-N(5)=127.7° (symmetric code #2: $1+x$, $-1+y$, $1+z$ and #3: $1+x$, y, $1+z$). The H-bonding interactions between the anions and the cations lead to the formation of two dimensional molecular sheet, such a molecular layer is parallel to the crystallographic (10-1) plane, and the adjacent H-

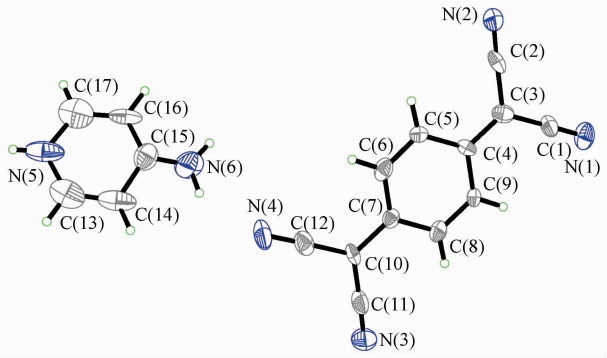

Fig.1 ORTEP view of **1** with thermal ellipsoids at 30% probability level.

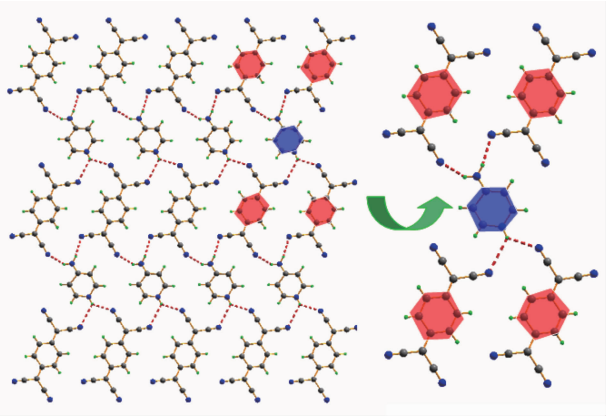

Fig.2 Two dimensional molecular sheet formed via H-bonding interaction between anions and cations parallel to the crystallographic (10-1) plane

Table 2 Mean bond lengths (nm) of the TCNQ molecules in 1

Labeling system is illustrated below

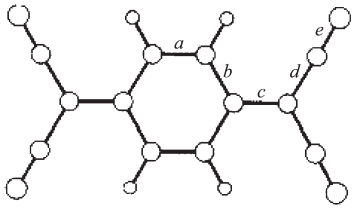

	a	*b*	*c*	*d*	*e*	*c*/(*b*+*d*)
TCNQ in **1**	0.136 7(4)	0.141 2(4)	0.140 2(4)	0.142 8(5)	0.114 2(5)	0.521
TCNQ[0][28]	0.134 6	0.144 8	0.137 4	0.144 0	0.113 8	0.475
$TCNQ^{-1/2}$[27]	0.135 5	0.143 3	0.139 6	0.142 4	0.114 5	0.488
$TCNQ^{-1}$[26]	0.136 2	0.142 4	0.141 3	0.141 7	0.114 9	0.497

bonding molecular layers exhibit *a* typical arrangement of slip form along the crystallographic *a*+*c* direction, which gives rise to the formation of mixed stacks with *a* manner of ...AACCAACC... along the a-axis with *a* much smaller separation of 0.3072 nm between the mean molecular planes of AA (cf. Fig.3 and Scheme 2); the adjacent slipping H-bonding layers are held together via van der Waals forces.

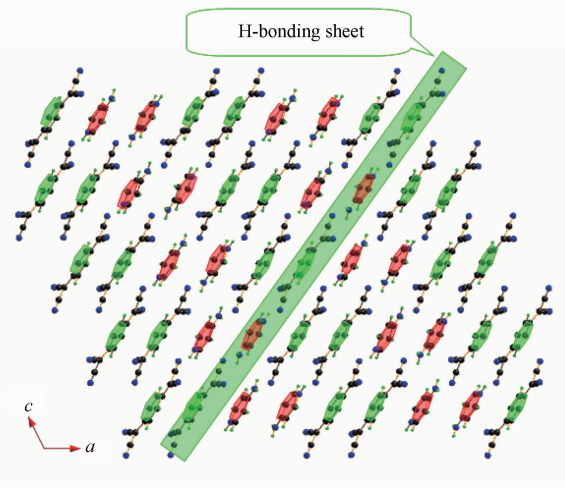

Fig.3 Packing diagram of **1** projected along b-axis showing the mixed stacks of anions (A) and cations (C) in the fashion of ...AACCAACC... along the direction of a-axis as well as the molecular sheets via H-bonding interactions parallel to the crystallographic (10-1) plane

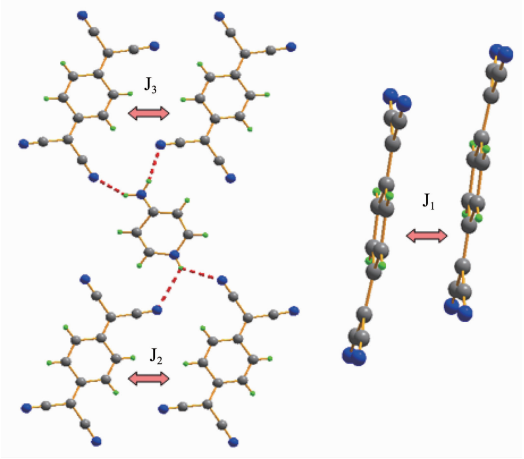

Scheme 2 Illustrations of each spin dimer (magnetic exchange constant *J* is calculated in the crystal of **1**)

2.2 Magnetic susceptibilities and broken symmetry analysis

The sample for magnetic measurement was examined by powder X-ray diffraction (PXRD) technique, and the experimental and simulated profiles are given in Fig.4, which indicates the sample has high purity. The plot of molar magnetic susceptibility (χ_m) variations with temperature for **1** is displayed in Fig.5. One can see that this compound is almost diamagnetism in the temperature range of 2~400 K. In accordance to the analysis of the crystal structure, the paramagnetic $TCNQ^-$ ions exist in an isolated π-type dimeric form, and the neighboring π-type $(TCNQ)_2^{2-}$ dimers are connected together via 4-NH_2-Py^+ cations by intermolecular H-bonding interactions on the H-bonding layers. As a result, there should be strong antiferromagnetic exchange interaction within a π-type $(TCNQ)_2^{2-}$ dimer, and such a kind of spin-paired (singlet) ground states is also observed in crystalline salts of the anion-radical salts derived from the related electron acceptor

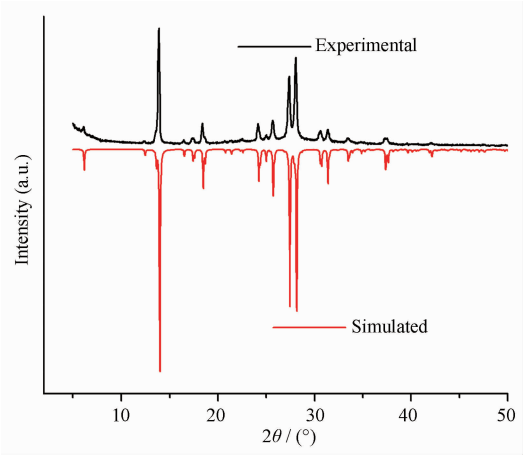

Fig.4 Experimental and simulated XRD patterns for **1**

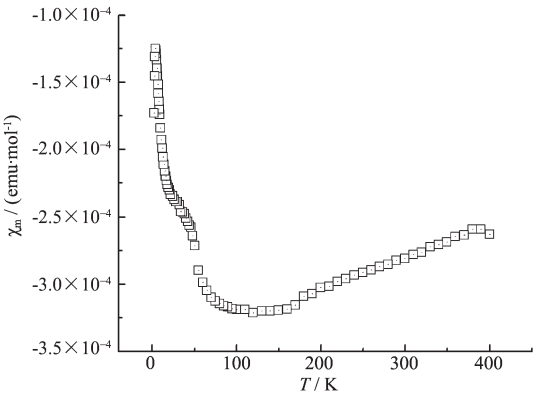

Fig.5 Molar magnetic susceptibility (χ_m) of **1** as a function of temperature

tetracyanoquinodimethane[30-31].

In order to gain a deeper understanding of the magnetic behavior for **1**, the broken-symmetry DFT approach was employed to evaluate the magnetic exchange constants. The broken symmetry formalism, originally developed by Noodleman for SCF methods [32], which involves a variational treatment within the restrictions of a single spin-unrestricted Slater determinant built upon using different orbitals for different spin. This approach has been later applied within the framework of DFT as a practical tool to investigate magnetic interactions on rather large systems (for example, polynuclear, 1D, 2D and 3D spin systems)[33-36] with reasonable accuracy and partial consideration of electron correlation effects [37-38]. For the possible pathways in **1**, the calculated energies for the high-spin triplet and broken-symmetry (BS) states of the spin dimers associated with the spin exchange paths (i.e., structural units consisting of two adjacent magnetic anion sites) are combined to estimate the exchange constant J involved in the widespread used Heisenberg-Dirac-van Vleck Hamiltonian[39-41]:

$$\hat{H} = -2J\vec{S}_1\vec{S}_2 \quad (\mathbf{1})$$

where $\vec{S}_1$ and $\vec{S}_2$ are the respective spin angular momentum operators, J is the magnetic exchange constant between two coupled magnetic centers. A positive sign of J indicates a ferromagnetic (FM) interaction, whereas the negative sign shows an AFM interaction. Assuming the so-called "weak bonding" regime, Noodleman et al.[42] evaluated J values within broken symmetry framework by

$$J = \frac{E_{BS} - E_T}{S_{max}^2} \quad (\mathbf{2})$$

where E_{BS} and E_T denote the total energies in the broken symmetry (BS) singlet state and triplet state, respectively, and S_{max} corresponds to the total spin of the high-spin state. It has been suggested that the following expression might give more reasonable solutions in the strong overlap region[43-44]:

$$J^{(2)} = \frac{E_{BS} - E_T}{S_{max}(S_{max}+1)} \quad (\mathbf{3})$$

However, Yamag uc hi et al. claimed that J obtained by the approximate spin projection procedure reproduces the characteristic feature of J in the whole region[37,45]:

$$J^{(3)} = \frac{E_{BS} - E_T}{\langle S^2\rangle_T - \langle S^2\rangle_{BS}} \quad (\mathbf{4})$$

and the $\langle S^2\rangle_T$ and $\langle S^2\rangle_{BS}$ in Eq. (**4**) denote the total spin angular momentum of triplet state and broken-symmetry singlet state, respectively. Each spin dimer, with calculated magnetic exchange constant is demonstrated in Scheme 2 for **1**, and the calculated $\langle S^2\rangle_T$ and $\langle S^2\rangle_{BS}$ values as well as the J values obtained from Eq. (**2**) to Eq. (**4**) are summarized in Table 3. The calculations indicate the existence of strong AFM coupling within the face-to-face stacking $(TCNQ)_2^{2-}$ dimer, and the magnetic exchange interactions between the neighboring $TCNQ^-$ anions linked via hydrogen bond could be neglected. As a result, the big energy gap between the nonmagnetic singlet state and the thermally activated triplet state within the face-to-face stacking $(TCNQ)_2^{2-}$ dimer leads to the existence of the ignorable population of the spin-triplet state, and **1** exhibits almost the characteristics of diamagnetism.

Table 3 Calculated $\langle S^2\rangle_T$ and $\langle S^2\rangle_{BS}$ as well as J values for each spin dimer in 1

Spin dimer	$J^{(1)}/k_B$ / K	$J^{(2)}/k_B$ / K	$J^{(3)}/k_B$ / K	$\langle S^2\rangle_T$	$\langle S^2\rangle_{BS}$
J_1	−3 620.3	−1 810.2	−1 805.1	2.005 6	0.000 0
J_2	−0.9	−0.5	−0.9	2.005 6	1.005 1
J_3	0.9	0.5	0.9	2.005 6	1.005 1

3 Conclusions

In summary, we prepared a new ion-pair compound containing paramagnetic $TCNQ^-$ and nonmagnetic 4-aminopyridinium. Its single crystal structure shows the existence of isolated π-type of $(TCNQ)_2^{2-}$ dimers with much smaller distance of mean molecular planes (0.3072 nm), and the adjacent $(TCNQ)_2^{2-}$ dimers are connected

by 4-aminopyridinium via strong hydrogen bonds. The variable temperature magnetic susceptibility measurement discloses that this ion-pair compound is almost diamagnetism in the temperature range of 2~400 K, and the theoretical analysis further reveals that this diamagnetism behavior arises from the existence of strong AFM coupling interaction within the π-type of $(TCNQ)_2^{2-}$ dimer and the big energy gap between nonmagnetic singlet state and the excited triplet state leads to the existence of ignorable population of excited triplet state.

References:

[1] Jain R, Kabir K, Gilroy J B, et al. *Nature*, **2007**,**445**:291-294

[2] Ferlay S, Mallah T, Ouahès R, et al. *Nature*, **1995**,**378**:701-703

[3] Manriquez J M, Yee G T, McLean R S, et al. *Science*, **1991**, **252**:1415-1417

[4] Ishii N, Okamura Y, Chiba S, et al. *J. Am. Chem. Soc.*, **2008**,**130**:24-25

[5] Nihei M, Tahira H, Takahashi N, et al. *J. Am. Chem. Soc.*, **2010**,**132**:3553-3560

[6] Itkis M E, Chi X, Cordes A W, et al. *Science*, **2002**,**296**:1443-1445

[7] Coronado E, Galán-Mascarós J R, Gómez-Garía C J, et al. *Nature*, **2000**,**408**:447-449

[8] Komatsu H, Matsushita M M, Yamamura S, et al. *J. Am. Chem. Soc.*, **2010**,**132**:4528-4529

[9] Sessoli R, Gatteschi D, Caneschi A, et al. *Nature*, **1993**,**365**:141-143

[10]Aubin S M J, Sun Z, Pardi L, et al. *Inorg. Chem.*, **1999**,**38**:5329-5340

[11]Caneschi A, Gatteschi D, Lalioti N, et al. *Angew. Chem. Int. Ed.*, **2001**,**40**:1760-1763

[12]Duan H B, Ren X M, Meng Q J. *Coord. Chem. Rev.*, **2010**, **254**:1509-1522

[13]Ren X M, Nishihara S, Akutagawa T, et al. *Inorg. Chem.*, **2006**,**45**:2229-2234

[14]Ren X M, Chen Y C, He C, et al. *J. C. S. Dolton Trans.*, **2002**:3915-3918

[15]Melby L R, Harder R J, Hertler W R, et al. *J. Am. Chem. Soc.*, **1962**,**84**:3374-3387

[16]Carlin R L. *Magnetochemistry*. Berlin Heidelberg: Springer-Verlag Publisher, **1986**:3

[17]Sheldrick G M. *SHELXL*-97. *Program for Crystal Structure Refinement*, University of Güttingen: Güttingen, Germany, **1997**.

[18]Frisch M J, Trucks G. W, Schlegel H B, et al. *Gaussian* 98, *Revision* A.11, Gaussian, Inc., Pittsburgh, PA, USA **2001**.

[19]Hohenberg P, Kohn W. *Phys. Rev.*, **1964**,**136**:B864-B871

[20]Kohn W, Sham L J. *Phys. Rev.*, **1965**,**140**:A1133-A1138

[21]Becke A D. *Phys. Rev. A*, **1988**,**38**:3098-3100

[22]Perdew J P, Burke K, Wang Y. *Phys. Rev. B*, **1996**,**54**:16533-16539

[23]Becke A D. *J. Chem. Phys.*, **1993**,**98**:5648-5652

[24]Lee C, Yang W, Parr R G. *Phys. Rev. B*, **1988**,**37**:785-789

[25]Liu G X, Ren X M, Kremer R K, et al. *J. Mol. Struct.*, **2005**,**743**:125-133

[26]Ashwell G J, Eley D D, Harper A, et al. *Acta Cryst. B*, **1977**,**33**:2258-2263

[27]Ashwell G J, Wallwork S C, Barker S R, et al. *Acta Cryst. B*, **1975**,**31**:1175-1178

[28]Long R E, Sparks R A, Trueblood K N. *Acta Cryst.*, **1965**, **18**:932-939

[29]Flandrois P S, Chasseau D. *Acta Cryst. B*, **1977**,**33**:2744-2750

[30]Lü J M, Rosokha S V, Kochi J K. *J. Am. Chem. Soc.*, **2003**, **125**:12161-12171

[31]Miller J S, Zhang J H, Reiff W M, et al. *J. Phys. Chem.*, **1987**,**91**:4344-4360

[32]Noodleman L, Norman J G Jr. *J. Chem. Phys.*, **1979**,**70**:4903-4906

[33]Singh R, Banerjee A, Colacio E, et al. *Inorg. Chem.*, **2009**, **48**:4753-4762

[34]Manson J L, Conner M M, Schlueter J A. *Chem. Mater.*, **2008**,**20**:7408-7416

[35]Manson J L, Schlueter J A, Funk K A, et al. *J. Am. Chem. Soc.*, **2009**,**131**:6733-6747

[36]Mitsumi M, Yoshida Y, Kohyama A, et al. *Inorg. Chem.*, **2009**,**48**:6680-6691

[37]Nagao H, Nishino M, Shigeta Y, et al. *Coord. Chem. Rev.*, **2000**,**198**:265-295

[38]Ciofini I, Daul C A. *Coord. Chem. Rev.*, **2003**,**187**:238-239

[39]Heisenberg W. *Z. Phys.*, **1928**,**49**:619-636

[40]Dirac P A M. *The Principles of Quantum Mechanics*. Oxford: Clarendon Press, **1947**.

[41]Van Vleck J H. *The Theory of Electric and Magnetic Susceptibilities*. Oxford: Oxford University Press, **1932**.

[42]Noodleman L, Davidson E R. *Chem. Phys.*, **1986**,**109**:131-143

[43]Bencini A, Totti F, Daul C A, et al. *Inorg. Chem.*, **1997**,**36**:5022-5030

[44]Ruiz E, Cano J, Alvarez S, et al. *J. Comput. Chem.*, **1999**, **20**:1391-1400

[45]Takano Y, Kitagawa Y, Onishi T, et al. *J. Am. Chem. Soc.*, **2002**,**124**:450-461